Product Datasheet

LAP (TGF-beta 1) Antibody (7F6) - BSA Free
NBP2-22114

Unit Size: 0.1 ml

Store at 4C short term. Aliquot and store at -20C long term. Avoid freeze-thaw cycles.

www.novusbio.com technical@novusbio.com

Reviews: 3 Publications: 21

Protocols, Publications, Related Products, Reviews, Research Tools and Images at:
www.novusbio.com/NBP2-22114

Updated 9/9/2025 v.20.1

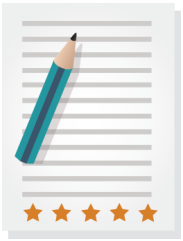

NBP2-22114

LAP (TGF-beta 1) Antibody (7F6) - BSA Free

Product Information

Unit Size	0.1 ml
Concentration	1 mg/ml
Storage	Store at 4C short term. Aliquot and store at -20C long term. Avoid freeze-thaw cycles.
Clonality	Monoclonal
Clone	7F6
Preservative	0.02% Sodium Azide
Isotype	IgG1
Purity	Ammonium sulfate precipitation
Buffer	PBS
Target Molecular Weight	44.3 kDa

Product Description

Description	Novus Biologicals Mouse LAP (TGF-beta 1) Antibody (7F6) - BSA Free (NBP2-22114) is a monoclonal antibody validated for use in IHC, WB, ELISA and Flow. Anti-LAP (TGF-beta 1) Antibody: Cited in 18 publications. All Novus Biologicals antibodies are covered by our 100% guarantee.
Host	Mouse
Gene ID	7040
Gene Symbol	TGFB1
Species	Human, Mouse, Rat
Reactivity Notes	Mouse reactivity reported in scientific literature (PMID: 26851347). Rat reactivity reported in scientific literature (PMID: 30147399).
Immunogen	Purified recombinant fragment of human TGF beta 1 (amino acids 62-197) expressed in E. coli. [UniProt# P01137]

Product Application Details

Applications	Western Blot, Immunohistochemistry-Paraffin, ELISA, Flow Cytometry, Immunohistochemistry
Recommended Dilutions	Western Blot 1:500-1:2000, Flow Cytometry 1:200-1:400, ELISA 1:10000, Immunohistochemistry reported in scientific literature (PMID 30147399), Immunohistochemistry-Paraffin reported by customer review

Images

Western Blot: LAP (TGF-beta 1) Antibody (7F6) [NBP2-22114] - Western blot analysis using TGF beta 1 mAb against human LAP (TGF-beta 1) recombinant protein. (Expected MW is 41 kDa)

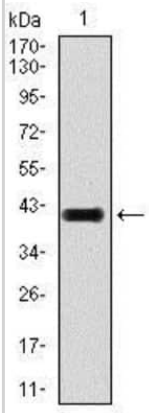

Immunohistochemistry-Paraffin: LAP (TGF-beta 1) Antibody (7F6) [NBP2-22114] - Immunohistochemical analysis of paraffin-embedded lymphoid tissue tissues using LAP (TGF-beta 1) mouse mAb with DAB staining.

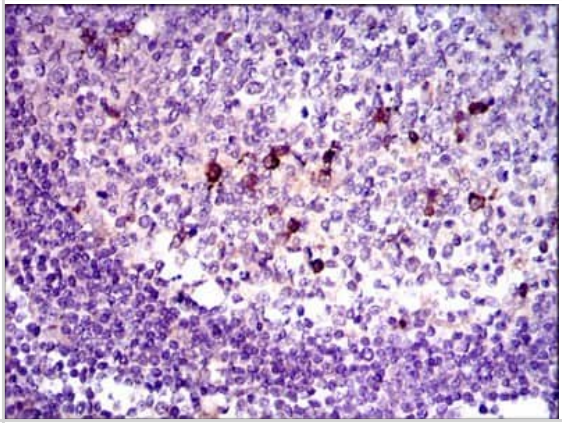

Flow Cytometry: LAP (TGF-beta 1) Antibody (7F6) [NBP2-22114] - Flow cytometric analysis of A549 cells using LAP (TGF-beta 1) mouse mAb (green) and negative control (red).

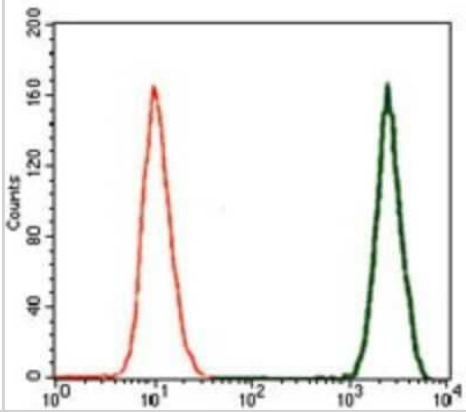

Western Blot: LAP (TGF-beta 1) Antibody (7F6) [NBP2-22114] - Western blot analysis of human stomach tissue (A) and human small intestine tissue (B) using TGF beta 1 antibody (NBP2-22114) at 2 ug/ml.

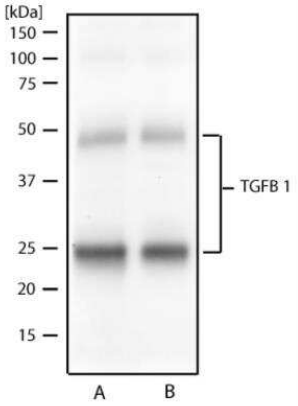

Immunohistochemistry-Paraffin: LAP (TGF-beta 1) Antibody (7F6) [NBP2-22114] - Human tonsil. Image from verified customer review.

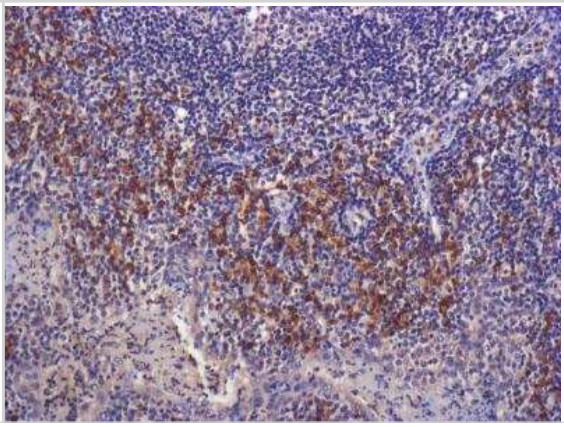

Immunohistochemistry-Paraffin: LAP (TGF-beta 1) Antibody (7F6) [NBP2-22114] - Immunohistochemical analysis of paraffin-embedded lung cancer tissues using LAP (TGF-beta 1) mouse mAb with DAB staining.

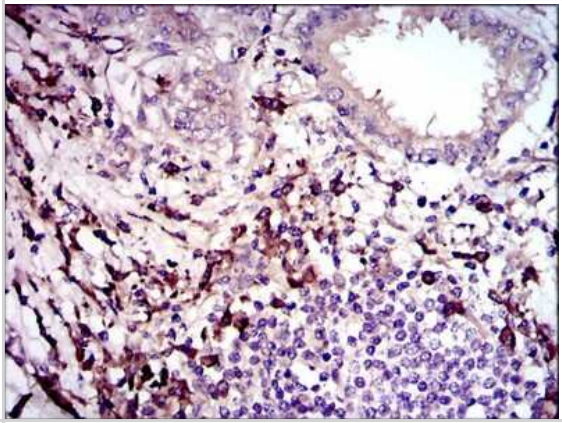

ELISA: LAP (TGF-beta 1) Antibody (7F6) [NBP2-22114] - Red: Control Antigen (100ng); Purple: Antigen (10ng); Green: Antigen (50ng); Blue: Antigen (100ng).

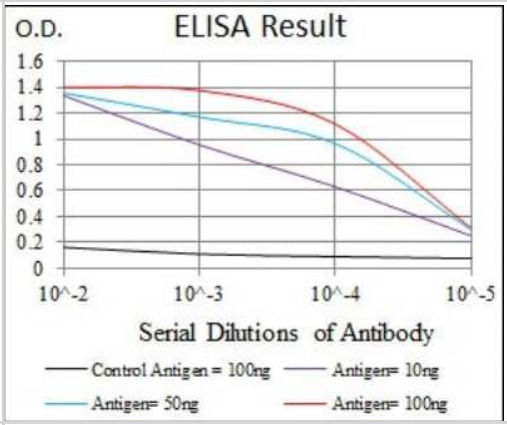

CD47 regulates thrombospondin-1, TGF-β1, and collagen deposition after injury. a Whole cell lysates from freshly isolated intestinal epithelial cells from Cd47f/f and Cd47ΔIEC mice were subjected to SDS–PAGE and immunoblot for thrombospondin-1/TSP-1, TGF-β1, and phosphorylated SMAD2 and SMAD3. Results are representative of three independent experiments. b Representative Masson's trichrome staining of wounds beds and chronic DSS-colitis colons from Cd47f/f and Cd47ΔIEC mice. Scale bars = 50 μm. Results representative of three independent experiments with 5–7 mice per group. Source data are provided as a Source Data file Image collected and cropped by CiteAb from the following open publication (https://pubmed.ncbi.nlm.nih.gov/31676794), licensed under a CC-BY license. Not internally tested by Novus Biologicals.

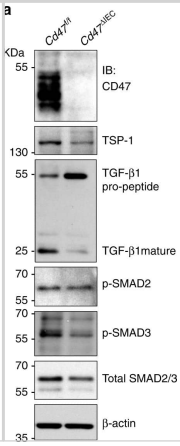

Inhibition of ERK1/2 activation attenuates myocardial remodeling and inflammation in permanent MI.Trametinib- and vehicle-treated mice were studied for 7 days after permanent LAD ligation. (A) Relative mRNA expression analysis of Il6, Tnf, Ccl2, and Ccr2 from the infarcted myocardium. (B) Flow cytometry analysis of the infarcted myocardium obtained from vehicle- or trametinib-treated mice normalized to heart weight. Representative gating strategies for quantification of CD45+ leukocytes: CD45+CD90.2–B220–NK1.1–CD11b+ myelomonocytic cells, CD45+CD90.2–B220–NK1.1–CD11b+Ly6G–F4/80–Ly6Chi monocytes, and CD45+CD90.2–B220–NK1.1–CD11b+Ly6G–F4/80–Ly6Clo macrophages. (C) Protein expression analysis of p-ERK1/2 (normalized to total ERK1/2) and activated TGF-β1 (normalized to GAPDH) in infarcted myocardium obtained from vehicle- or trametinib-treated mice. IOD, integrated optical density. (D) Protein expression analysis of p-ERK1/2 (normalized to ERK1/2) and activated TGF-β1 (normalized to GAPDH) in PBMCs isolated from vehicle- or trametinib-treated mice. Ordinary 1-way ANOVA, Šidak's multiple-comparison test; n = 4–6 animals per group. Data are shown as mean +/- SEM. *P < 0.05, **P < 0.01, ***P < 0.001, ****P < 0.0001. Image collected and cropped by CiteAb from the following open publication (https://pubmed.ncbi.nlm.nih.gov/36548062), licensed under a CC-BY license. Not internally tested by Novus Biologicals.

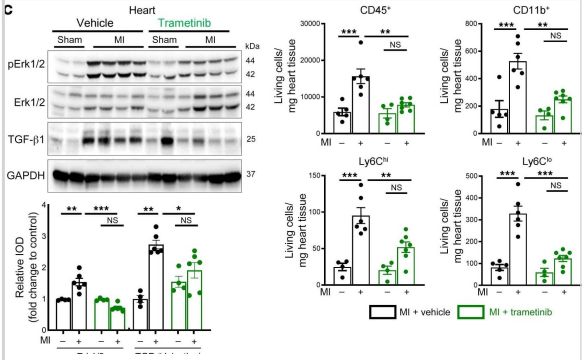

Inhibition of ERK1/2 activation attenuates myocardial remodeling and inflammation in permanent MI.Trametinib- and vehicle-treated mice were studied for 7 days after permanent LAD ligation. (A) Relative mRNA expression analysis of Il6, Tnf, Ccl2, and Ccr2 from the infarcted myocardium. (B) Flow cytometry analysis of the infarcted myocardium obtained from vehicle- or trametinib-treated mice normalized to heart weight. Representative gating strategies for quantification of CD45+ leukocytes: CD45+CD90.2–B220–NK1.1–CD11b+ myelomonocytic cells, CD45+CD90.2–B220–NK1.1–CD11b+Ly6G–F4/80–Ly6Chi monocytes, and CD45+CD90.2–B220–NK1.1–CD11b+Ly6G–F4/80–Ly6Clo macrophages. (C) Protein expression analysis of p-ERK1/2 (normalized to total ERK1/2) and activated TGF-β1 (normalized to GAPDH) in infarcted myocardium obtained from vehicle- or trametinib-treated mice. IOD, integrated optical density. (D) Protein expression analysis of p-ERK1/2 (normalized to ERK1/2) and activated TGF-β1 (normalized to GAPDH) in PBMCs isolated from vehicle- or trametinib-treated mice. Ordinary 1-way ANOVA, Šidak's multiple-comparison test; n = 4–6 animals per group. Data are shown as mean +/- SEM. *P < 0.05, **P < 0.01, ***P < 0.001, ****P < 0.0001. Image collected and cropped by CiteAb from the following open publication (https://pubmed.ncbi.nlm.nih.gov/36548062), licensed under a CC-BY license. Not internally tested by Novus Biologicals.

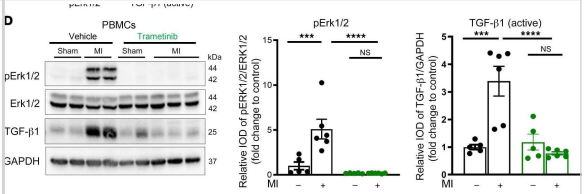

The upregulation of TGFβ1/IGF-1/BDNF expression in the brain of AD mice by PBMT extended to promote adult hippocampal neurogenesis. A, B Western blotting analysis (A) and quantification (B) of TGFβ1/IGF-1/BDNF expression in APP/PS1 and 3xTg-AD mouse brain after PBMT, (n = 3–4 per group). C The concentration of TGFβ1/IGF-1/BDNF in brain tissues were measured by enzyme linked immunosorbent assay (ELISA), (n = 3–6 per group). D Representative images of Nestin+ (neural stem cell staining) and neuronal class-III β-tubulin (Tuj1)+ (newborn neurons staining) expression cells in APP/PS1 and 3xTg-AD mouse hippocampal dentate gyrus (DG) at the end of PBMT. Scale bars, 50 μm. E Quantitative analyses of Nestin+ and Tuj1+ area in the hippocampal DG of each group, (n = 4 per group). F Quantitative analyses of the Nestin and Tuj1 mean fluorescence (MFI) in the brain tissues of each group after PBMT. The Nestin and Tuj1 MFI were detected by flow cytometer, (n = 5–6 per group). G Tuj1 antibody was used to staining the newborn neurons, and then, the expression of α-amino-3-hydroxy-5-methyl-4-isoxazole-propionic acid receptors (AMPAR) and postsynaptic density protein 95 (PSD95) on Tuj1+ neurons were detected by flow cytometer. All quantifications are presented as mean +/- SEM and were analyzed by one-way ANOVA test; ***p < 0.001, **p < 0.01, *p < 0.05 versus WT group; ###p < 0.001, ##p < 0.01, #p < 0.05 versus indicated group Image collected and cropped by CiteAb from the following open publication (https://pubmed.ncbi.nlm.nih.gov/36217178), licensed under a CC-BY license. Not internally tested by Novus Biologicals.

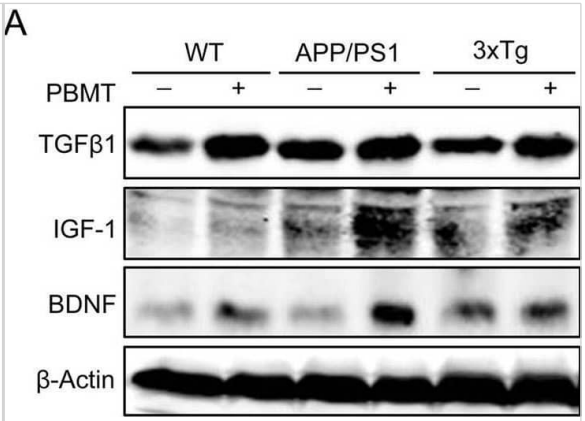

TF cytoplasmic domain phosphorylation–dependent increased TGF-β1 activation in clinical setting of MI.(A) Representative confocal images of phosphorylation status of TF in infarcted myocardium obtained from WT or TFΔCT mice after 7 days. Representative images and quantification of biological replicates. Kruskal-Wallis test and Dunn's multiple-comparison test; n = 3–4 animals per group. Scale bars: 50 μm. (B) Representative immunofluorescence confocal microscopy images of CD45+ and CD45/p-TF double-positive cells in human myocardium specimens obtained from n = 5 nonischemic (NI) donor hearts and n = 7 IHF patients. Quantification of biological replicates. Mann-Whitney test. Scale bars: 50 μm. (C and D) Western blot analysis and quantification of human LV tissue obtained from n = 5 nonischemic donor hearts and n = 9 IHF patients for p-TF (normalized to total TF) and TF (C) or TGF-β1 (normalized to GAPDH) and p-SMAD2 (normalized to total SMAD2) (D). Mann-Whitney test. Data are shown as mean +/- SEM. *P < 0.05. Image collected and cropped by CiteAb from the following open publication (https://pubmed.ncbi.nlm.nih.gov/36548062), licensed under a CC-BY license. Not internally tested by Novus Biologicals.

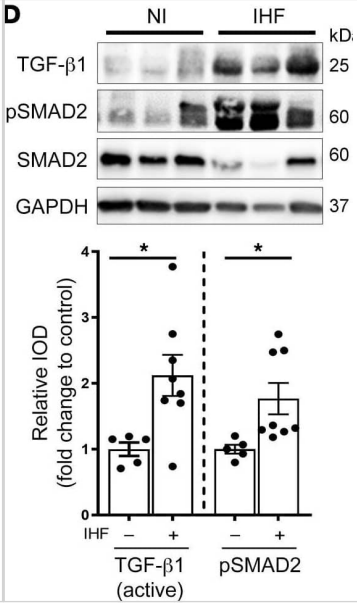

A profibrotic MEK1/2–TGF-β1 pathway is linked to PAR2-mediated ROS signaling in monocytes.(A and B) Protein expression analysis of monocytes isolated from WT mice and pretreated in vitro with trametinib (10 μM) for 1 hour (A), or isolated from PAR2–/– versus WT mice (B). Cells were stimulated with an inflammatory cytokine cocktail containing IL-6, TNF-α, and CCL2 at a concentration of 20 ng/mL with and without hypoxia for 4 hours. Western blotting of p-ERK1/2 (normalized to total ERK1/2) and activated TGF-β1 (normalized to GAPDH). Ordinary 1-way ANOVA, Šidak's multiple-comparison test; n = 5 replicates (2–3 mice were pooled for each sample). (C–E) PAR2fl/fl and PAR2fl/fl LysMCre littermates were subjected to permanent LAD ligation and investigated after 7 days; n = 5–10 animals per group. (C) Western blot analysis of activated TGF-β1 (normalized to GAPDH) and p-SMAD2 (normalized to total SMAD2) in the infarcted myocardium. Representative blots and quantification of biological replicates. (D) High-frequency ultrasound echocardiography obtained from PAR2fl/fl LysMCre and PAR2fl/fl littermate control mice with measurement of LVEF (%) and LVEDV (μL). Mann-Whitney test. (E) Kaplan-Meier survival analysis of permanently LAD-ligated PAR2fl/fl LysMCre and PAR2fl/fl littermate control mice over 7 days. Log-rank (Mantel-Cox) test. (F) Sirius red staining and deconvoluted images of fibrotic area on paraffin-embedded heart sections 4 weeks after permanent LAD ligation to induce IHF. Representative images and quantification of fibrotic areas normalized to surface area. Unpaired, 2-sided t test; n = 5 animals per group. Data are shown as mean +/- SEM. *P < 0.05, **P < 0.01, ****P < 0.0001. Image collected and cropped by CiteAb from the following open publication (https://pubmed.ncbi.nlm.nih.gov/36548062), licensed under a CC-BY license. Not internally tested by Novus Biologicals.

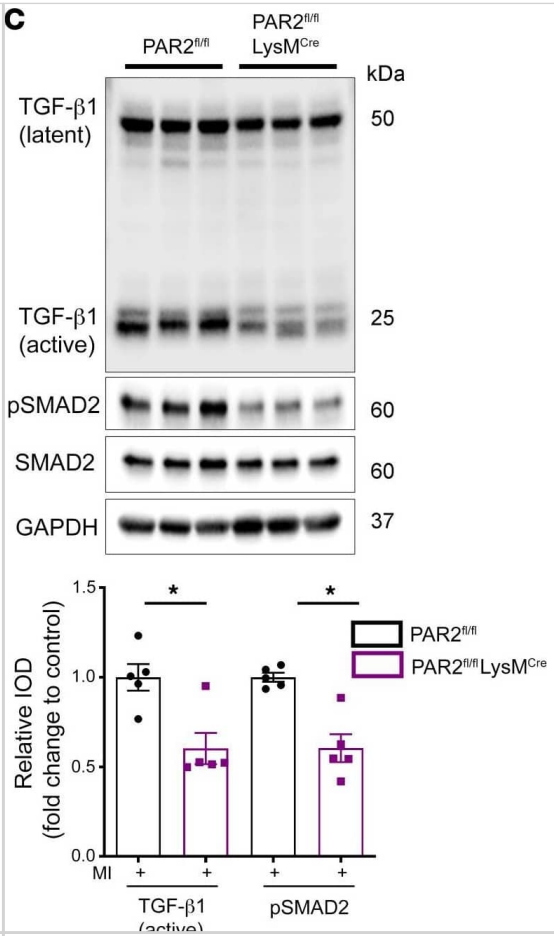

A profibrotic MEK1/2–TGF-β1 pathway is linked to PAR2-mediated ROS signaling in monocytes.(A and B) Protein expression analysis of monocytes isolated from WT mice and pretreated in vitro with trametinib (10 μM) for 1 hour (A), or isolated from PAR2–/– versus WT mice (B). Cells were stimulated with an inflammatory cytokine cocktail containing IL-6, TNF-α, and CCL2 at a concentration of 20 ng/mL with and without hypoxia for 4 hours. Western blotting of p-ERK1/2 (normalized to total ERK1/2) and activated TGF-β1 (normalized to GAPDH). Ordinary 1-way ANOVA, Šidak's multiple-comparison test; n = 5 replicates (2–3 mice were pooled for each sample). (C–E) PAR2fl/fl and PAR2fl/fl LysMCre littermates were subjected to permanent LAD ligation and investigated after 7 days; n = 5–10 animals per group. (C) Western blot analysis of activated TGF-β1 (normalized to GAPDH) and p-SMAD2 (normalized to total SMAD2) in the infarcted myocardium. Representative blots and quantification of biological replicates. (D) High-frequency ultrasound echocardiography obtained from PAR2fl/fl LysMCre and PAR2fl/fl littermate control mice with measurement of LVEF (%) and LVEDV (μL). Mann-Whitney test. (E) Kaplan-Meier survival analysis of permanently LAD-ligated PAR2fl/fl LysMCre and PAR2fl/fl littermate control mice over 7 days. Log-rank (Mantel-Cox) test. (F) Sirius red staining and deconvoluted images of fibrotic area on paraffin-embedded heart sections 4 weeks after permanent LAD ligation to induce IHF. Representative images and quantification of fibrotic areas normalized to surface area. Unpaired, 2-sided t test; n = 5 animals per group. Data are shown as mean +/- SEM. *P < 0.05, **P < 0.01, ****P < 0.0001. Image collected and cropped by CiteAb from the following open publication (https://pubmed.ncbi.nlm.nih.gov/36548062), licensed under a CC-BY license. Not internally tested by Novus Biologicals.

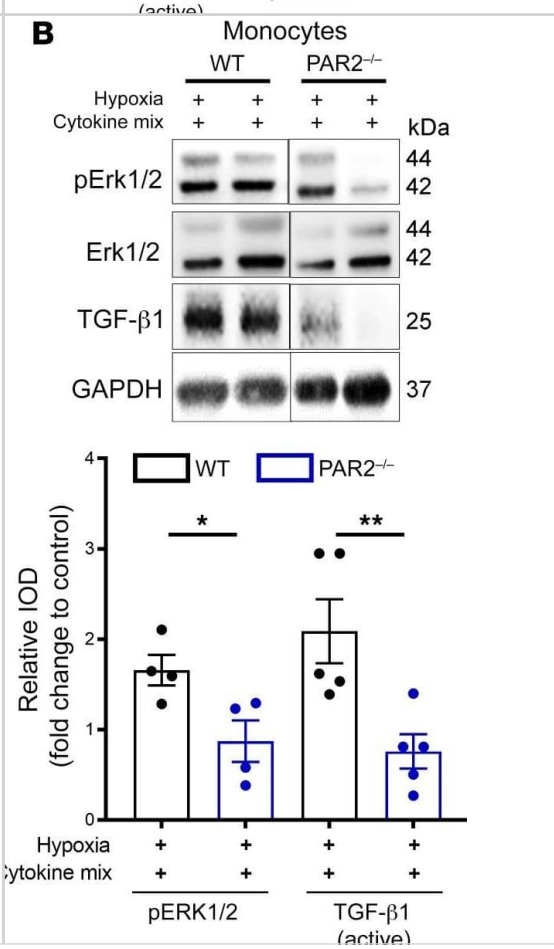

Myeloid cell–derived TF-PAR2 complex is required for TGF-β1 activation.(A) Confocal microscopy of myocardial cryosections obtained from n = 5 sham-operated and n = 5 LAD-ligated WT (C57BL/6J) mice at day 7. Representative images and quantification of TF+ cells costained for CD45. Unpaired, 2-sided t test. Scale bar: 50 μm. (B–D) TFfl/fl LysMCre and TFfl/fl littermates were subjected to permanent LAD ligation versus sham surgery and investigated after 7 days; n = 5–7 animals per group. (B) Protein expression analysis of p-ERK1/2 (normalized to total ERK1/2) in the infarcted myocardium. Ordinary 1-way ANOVA, Šidak's multiple-comparison test. (C) Western blot analysis of activated TGF-β1 (normalized to GAPDH) and p-SMAD2 (normalized to total SMAD2) in the infarcted myocardium obtained from TFfl/fl LysMCre and TFfl/fl littermates. Representative blots and quantification of biological replicates. (D) High-frequency ultrasound echocardiography obtained from TFfl/fl LysMCre and TFfl/fl littermates. Ordinary 1-way ANOVA, Šidak's multiple-comparison test. (E) Sirius red staining and deconvoluted images of fibrotic area on paraffin-embedded heart sections 4 weeks after permanent LAD ligation to induce IHF versus sham surgery. Representative images and quantification of fibrotic areas normalized to surface area. Ordinary 1-way ANOVA, Šidak's multiple-comparison test; n = 5 animals per group. (F) Kaplan-Meier survival analysis of permanently LAD-ligated TFfl/fl LysMCre and TFfl/fl littermate mice over 4 weeks. Log-rank (Mantel-Cox) test; n = 10–15 animals per group. Data are shown as mean +/- SEM. *P < 0.05, **P < 0.01, ***P < 0.001. Image collected and cropped by CiteAb from the following open publication (https://pubmed.ncbi.nlm.nih.gov/36548062), licensed under a CC-BY license. Not internally tested by Novus Biologicals.

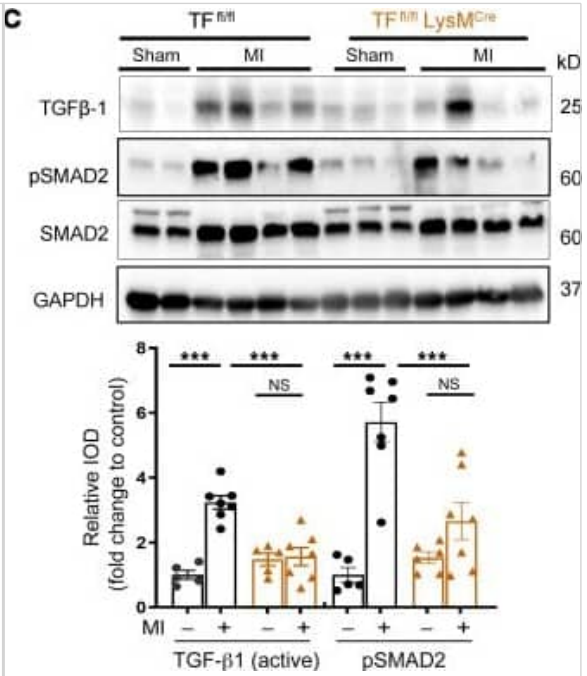

Myeloid cell TF cytoplasmic domain phosphorylation mediates ERK1/2–TGF-β1–dependent cardiac remodeling in permanent LAD ligation.(A) Confocal microscopy of myocardial cryosections obtained from WT (C57BL/6J) and TFΔCT mice. Representative images and quantification of MFI of Ly6C+TGFβ-1+ and CD31+TGF-β1+ cells. Ordinary 1-way ANOVA, Šidak's multiple-comparison test; n = 5 animals per group. Scale bars: 25 μm. (B) Mice with transplanted BM were subjected to permanent LAD ligation versus sham surgery and investigated 7 days later. Western blot analysis of NOX2 (normalized to GAPDH), p-ERK1/2 (normalized to total ERK1/2), and TGF-β1 (normalized to GAPDH) in infarcted myocardium obtained from chimeric mice. Ordinary 1-way ANOVA, Šidak's multiple-comparison test; n = 5–7 animals per group. Data are shown as mean +/- SEM. *P < 0.05, **P < 0.01, ***P < 0.001. Image collected and cropped by CiteAb from the following open publication (https://pubmed.ncbi.nlm.nih.gov/36548062), licensed under a CC-BY license. Not internally tested by Novus Biologicals.

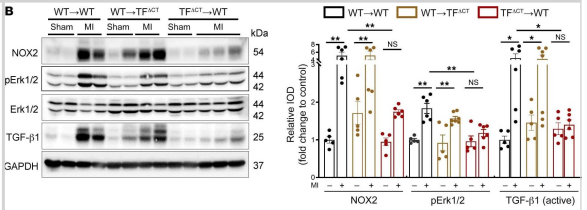

A profibrotic MEK1/2–TGF-β1 pathway is linked to PAR2-mediated ROS signaling in monocytes.(A and B) Protein expression analysis of monocytes isolated from WT mice and pretreated in vitro with trametinib (10 μM) for 1 hour (A), or isolated from PAR2–/– versus WT mice (B). Cells were stimulated with an inflammatory cytokine cocktail containing IL-6, TNF-α, and CCL2 at a concentration of 20 ng/mL with and without hypoxia for 4 hours. Western blotting of p-ERK1/2 (normalized to total ERK1/2) and activated TGF-β1 (normalized to GAPDH). Ordinary 1-way ANOVA, Šidak's multiple-comparison test; n = 5 replicates (2–3 mice were pooled for each sample). (C–E) PAR2fl/fl and PAR2fl/fl LysMCre littermates were subjected to permanent LAD ligation and investigated after 7 days; n = 5–10 animals per group. (C) Western blot analysis of activated TGF-β1 (normalized to GAPDH) and p-SMAD2 (normalized to total SMAD2) in the infarcted myocardium. Representative blots and quantification of biological replicates. (D) High-frequency ultrasound echocardiography obtained from PAR2fl/fl LysMCre and PAR2fl/fl littermate control mice with measurement of LVEF (%) and LVEDV (μL). Mann-Whitney test. (E) Kaplan-Meier survival analysis of permanently LAD-ligated PAR2fl/fl LysMCre and PAR2fl/fl littermate control mice over 7 days. Log-rank (Mantel-Cox) test. (F) Sirius red staining and deconvoluted images of fibrotic area on paraffin-embedded heart sections 4 weeks after permanent LAD ligation to induce IHF. Representative images and quantification of fibrotic areas normalized to surface area. Unpaired, 2-sided t test; n = 5 animals per group. Data are shown as mean +/- SEM. *P < 0.05, **P < 0.01, ****P < 0.0001. Image collected and cropped by CiteAb from the following open publication (https://pubmed.ncbi.nlm.nih.gov/36548062), licensed under a CC-BY license. Not internally tested by Novus Biologicals.

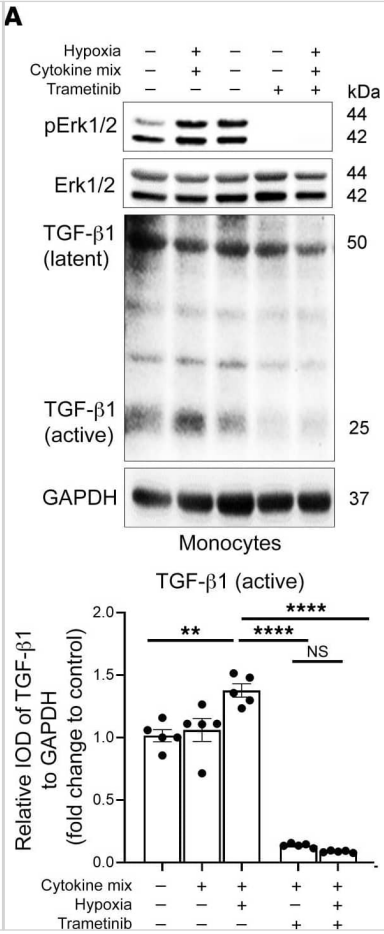

Publications

Abdelhady R, Sayed R, Younis N et al. Targeting JNK1/2 and P38 Mitogen□Activated Protein Kinases With Pazopanib Mitigates Bleomycin□Induced Lung Fibrosis Archiv der Pharmazie 2025-09-28 [PMID: 41017227]

Son M, Yim H, Lee Y et al. Pre- and Postnatal Fine Particulate Matter Exposure and Renal Fibrogenesis in Adult Male Rats: The Role of Vitamin D Supplementation. Current issues in molecular biology 2025-05-22 [PMID: 40699786]

Wu X, Shen Q, Chang H et al. Promoted CD4(+) T cell-derived IFN-?/IL-10 by photobiomodulation therapy modulates neurogenesis to ameliorate cognitive deficits in APP/PS1 and 3xTg-AD mice Journal of Neuroinflammation 2022-10-10 [PMID: 36217178]

Z Shen, W Luo, B Tan, K Nie, M Deng, S Wu, M Xiao, X Wu, X Meng, T Tong, C Zhang, K Ma, Y Liao, J Xu, X Wang Roseburia intestinalis stimulates TLR5-dependent intestinal immunity against Crohn's disease EBioMedicine, 2022-09-28;85(0):104285. 2022-09-28 [PMID: 36182776]

Lang M, Krump C, Meshcheryakova A et al. Microenvironmental and cell intrinsic factors governing human cDC2 differentiation and monocyte reprogramming Frontiers in Immunology 2023-07-19 [PMID: 37539048]

Garlapati V, Molitor M, Michna T et al. Targeting myeloid cell coagulation signaling blocks MAP kinase/TGF-?1-driven fibrotic remodeling in ischemic heart failure Journal of Clinical Investigation 2023-02-15 [PMID: 36548062]

Esmail MM, Saeed NM, Hanna DMF et Al. Hepatoprotective and neuroprotective effects of quinacrine against bile duct ligation-induced hepatic encephalopathy in rats: Role of bone morphogenetic proteins signaling Life Sci 2024-11-12 [PMID: 39537098]

Mousset A, Lecorgne E, Bourget I et al. Neutrophil extracellular traps formed during chemotherapy confer treatment resistance via TGF-? activation Cancer cell 2023-04-10 [PMID: 37037615] (WB, Mouse)

Mohamed MZ, Abed El Baky MF, Ali ME, Hafez HM Aprepitant exerts anti-fibrotic effect via inhibition of TGF-beta/Smad3 pathway in bleomycin-induced pulmonary fibrosis in rats Environmental toxicology and pharmacology 2022-08-02 [PMID: 35931359] (IHC-P, Rat)

Details:
1:100 IHC-P

Griffin J, Krolikowski J, Kounga K et al. Red Light Mitigates the Deteriorating Placental Extracellular Matrix in Late Onset of Preeclampsia and Improves the Trophoblast Behavior Journal of Pregnancy 2022-04-20 [PMID: 35494491] (IHC-Fr, Human)

Malik MNH, Waqas SFH, Zeitvogel J et al. Congenital deficiency reveals critical role of ISG15 in skin homeostasis The Journal of clinical investigation 2021-11-30 [PMID: 34847081] (IF/IHC, Human)

Sholqamy M TGF- beta Paradox and the Progression of Osteoblastoma versus Osteosarcoma. Egyptian Dental Journal 2021-10-01

More publications at http://www.novusbio.com/NBP2-22114

Novus Biologicals USA
10730 E. Briarwood Avenue
Centennial, CO 80112
USA
Phone: 303.730.1950
Toll Free: 1.888.506.6887
Fax: 303.730.1966
nb-customerservice@bio-techne.com

Bio-Techne Canada
21 Canmotor Ave
Toronto, ON M8Z 4E6
Canada
Phone: 905.827.6400
Toll Free: 855.668.8722
Fax: 905.827.6402
canada.inquires@bio-techne.com

Bio-Techne Ltd
19 Barton Lane
Abingdon Science Park
Abingdon, OX14 3NB, United Kingdom
Phone: (44) (0) 1235 529449
Free Phone: 0800 37 34 15
Fax: (44) (0) 1235 533420
info.EMEA@bio-techne.com

General Contact Information
www.novusbio.com
Technical Support: nb-technical@bio-techne.com
Orders: nb-customerservice@bio-techne.com
General: novus@novusbio.com

Products Related to NBP2-22114

NBP2-33376H	Blue Marker Antibody (6F4-F6) [HRP]
HAF007	Goat anti-Mouse IgG Secondary Antibody [HRP]
NB7539	Goat anti-Mouse IgG (H+L) Secondary Antibody [HRP]
NBP1-97005-0.5mg	Mouse IgG1 Isotype Control (MG1)

Limitations
This product is for research use only and is not approved for use in humans or in clinical diagnosis. Primary Antibodies are guaranteed for 1 year from date of receipt.

For more information on our 100% guarantee, please visit www.novusbio.com/guarantee

Earn gift cards/discounts by submitting a review: www.novusbio.com/reviews/submit/NBP2-22114

Earn gift cards/discounts by submitting a publication using this product: www.novusbio.com/publications